Int J Adv Manuf Technol (2016) 84:1757–1767
DOI 10.1007/s00170-015-7825-4

ORIGINAL ARTICLE

Tool path planning and machining deformation compensation in high-speed milling for difficult-to-machine material thin-walled parts with curved surface

Yuan-yuan Gao[1] · Jian-wei Ma[1] · Zhen-yuan Jia[1] · Fu-ji Wang[1] · Li-kun Si[1] · De-ning Song[1]

Received: 4 June 2015 / Accepted: 8 September 2015 / Published online: 21 September 2015

Abstract Difficult-to-machine material thin-walled parts with curved surface are widely used in industrial applications, and the shape accuracy is a basic requirement for ensuring the usability. Due to the low rigidity of the thin-walled curved surface parts, the cutting force becomes a sensitive factor for the machining deformation. In addition, high speed milling, that has an obvious attribute of small cutting force comparing with the traditional one, provides an effective way to process the thin-walled curved surface parts made by difficult-to-machine materials like titanium alloy. Moreover, the rigidity of the thin-walled curved surface parts is constantly changing along with the machining process, which leads to a more complex machining deformation when choosing different tool paths and affects the machining quality. To reduce the machining deformation, a proper cutting parameters combination which influences the machining deformation directly is obtained based on the established cutting force model, and then a deformation control strategy by planning tool path is put forward. At the same time, an efficient compensation method based on modifying cutter location point is proposed. Taking TC4 thin-walled arc-shaped parts as an example, experimental studies indicate that the largest deformation values reduce to 49 μm after compensation. Compared with the former 104 μm, the deformation degree decreases by 52.88 % when the thickness of the thin wall is 200 μm. The research provides an effective approach to reduce the machining deformation induced error for difficult-to-machine material thin-walled parts with curved surface.

Keywords Thin-walled · Curved surface · Difficult-to-machine materials · High speed milling · Machining deformation · Tool path · Deformation compensation

1 Introduction

Plenty of difficult-to-machine material thin-walled parts with curved surface are used in the aerospace industry because of their superior properties such as light weight, good corrosion resistance, and high heat resistance [1]. However, the thin thickness results in the reduction of rigidity severely which makes the machining deformation increase significantly. Besides, along with the machining process, the rigidity is changing all the time which leads to the cutting flutter and causes a more complex machining deformation. The deformation mostly does no good to the usability of the thin-walled parts [2]. Moreover, the harsh working condition in aerospace industry leads the thin-walled curved surface parts to be made by difficult-to-machine materials [3], such as blade [4], thin-walled curved surface workpiece [5], storage tank wall [6], etc, while the properties such as low Young modulus, low thermal conductivity, and high strength make the cutting force very large in the machining process when using traditional processing methods. As high-speed milling has the feature of small cutting force that makes it an appropriate method to manufacture the difficult-to-machine material, the high-speed milling technology for difficult-to-machine material thin-walled parts with curved surface has come to be a hotspot in the industry applications [7].

✉ Jian-wei Ma
mjw2011@dlut.edu.cn

[1] Key Laboratory for Precision and Non-traditional Machining Technology of the Ministry of Education, School of Mechanical Engineering, Dalian University of Technology, Dalian 116024, China

For difficult-to-machine material thin-walled parts with curved surface, the variation of geometric features leads to a difference for the rigidity of different positions of the parts. Meanwhile, the variation of rigidity caused by material removing process makes the deformation more complicated. In order to solve the problem of machining deformation in thin-walled parts machining, many researchers have given a lot for this field in the past few years. Some researchers focused on improving processing technology. Smith and Dvorak [8] presented a method of cutting on the full height layer by layer, after which several times no feed cutting were given to reduce the machining deformation and guarantee the shape accuracy whereas the efficiency was low. Iwabe et al. [9] proposed a method that processing with two parallel spindles which reduced the machining deformation effectively on account of force balance on both sides. However, a special machine tool with two parallel spindles was needed and there would be a requirement about the distance between two spindles, which made it unsuitable for using widely. Some researchers used certain algorithms to predict or compensate the machining deformation. Ratchev et al. [10] presented an integrated methodology for modeling and predicting the profile errors caused by deflection during machining of low-rigidity components and the flexible force was calculated by taking the changes of the engaged teeth immersion angles into account at each computational step. Chen et al. [11] established a dynamical model to predict the machining deformation in multilayer machining of a thin-walled part and the machining error was compensated at each layer by considering the error of the previous layer, which was proved to be an effectiveness method to reduce the machining deformation. Otherwise, a lot of researchers [12–18] devoted themselves to the study of machining deformation simulation so as to predict the deformation value of thin-walled parts. The prediction tests showed good agreement between simulation model and experimental data. Nonetheless, merely simulation process without compensation procedure is not enough, and more importantly, these studies are mostly aiming at slab thin-walled parts. However, there has not been much research done on the curved surface ones made by difficult-to-machine materials. Thus, an effective solving strategy for high-speed milling deformation reducing and compensation for difficult-to-machine material thin-walled parts with curved surface is urgently needed to be put forward.

Based on the above analysis, the purpose of the present application study is to find an efficient way to reduce the machining deformation for difficult-to-machine material thin-walled parts with curved surface. Aiming at this goal, a proper cutting parameters combination which influences the machining deformation directly is obtained based on the established cutting force model, which can reduce the cutting deformation, and then a deformation control strategy by tool path planning is put forward. At the same time, a compensation approach is also proposed after that to guarantee the shape precision of the thin-walled parts with curved surface. The research provides an effective method to reduce machining deformation for difficult-to-machine material thin-walled parts with curved surface.

2 Deformation reducing method in high-speed milling for difficult-to-machine material thin-walled parts with curved surface

As the machining deformation of the thin-walled curved surface parts is mainly caused by cutting force, the cutting force model is established at first for selecting an appropriate parameters combination which can reduce the machining deformation. Then, the impacts on machining deformation when processing with different tool paths are analyzed and a better tool path is planned. Afterwards, the finite element analysis method is adopted to simulate machining deformation under the cutting force calculated by the cutting force model. Meanwhile, a comparison between the actual deformation value and the simulated one is carried out, and what is more, a coefficient is obtained for predicting actual machining deformation. Finally, a compensation method is proposed to modify the cutter location points and validation experiments are conducted to proof the effectiveness of the proposed deformation error compensation method by taking TC4 arc-shaped thin-walled part as an example. The whole procedure is shown in Fig. 1. With this approach, commonly used machine tool is available and ordinary coating carbide milling tools can satisfy the cutting condition.

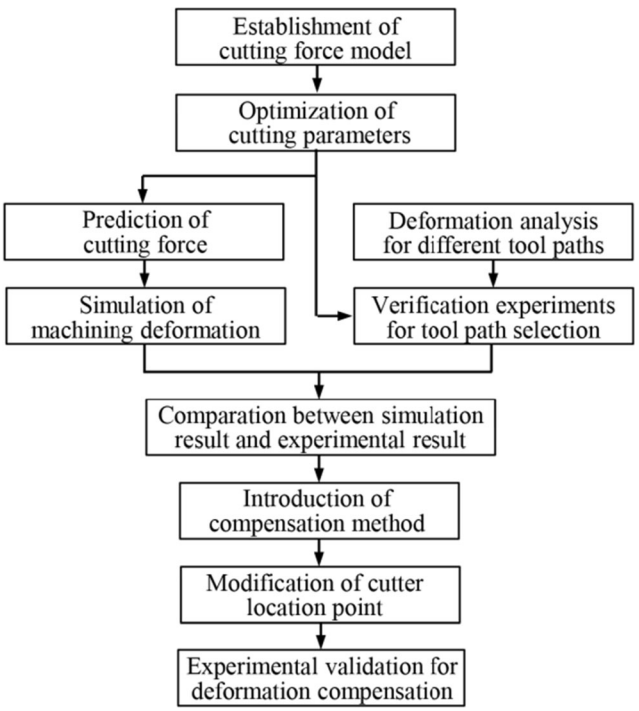

Fig. 1 Flow chart of the deformation reducing method

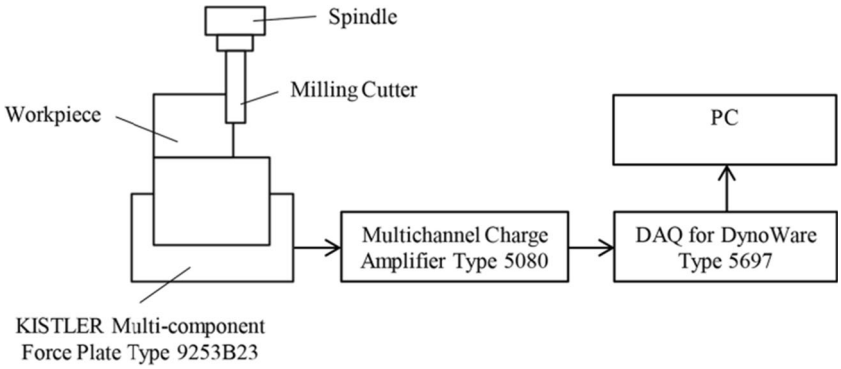

Fig. 2 Force measuring principle

3 Cutting parameter optimization and tool path planning for reducing machining deformation

In high-speed milling for difficult-to-machine material thin-walled parts with curved surface, it is of vital importance to select proper cutting parameter combination which influences the machining deformation directly. The cutting force model is established at first and then an optimization is conducted for selecting an appropriate parameters combination which can reduce the machining deformation. After that, the impacts on machining deformation when processing with different tool paths are analyzed and then the validation experiments are carried out for proving the analysis. Meanwhile, the finite element analysis method is adopted to do the simulation with the cutting force calculated by the cutting force model. Finally, a coefficient is obtained for predicting the actual machining deformation based on the simulated deformation value.

3.1 Experimental setup

The establishment of cutting force model should be set up by a series of experiments; thus, experiment should be set up at first. The details are as follows:

1. Machine tool. High-speed three-axis vertical milling machine tool MIKEON HSM 500 with HEIDENHAIN iTNC 530 NC system is adopted to conduct the processing. Its repeatability positioning accuracy is 5 μm, the machining precision is 0.1 μm, and the highest spindle speed can reach to 54,000 r min^{-1}.
2. Milling cutter. The cutting tools used are the POW R FEED M90 Series end mills coated cemented carbide tools with four flutes for high-performance milling, whose coating composition is AlGrN. The recommended cutting speed is within 150 m min^{-1}. The length of cut and the tool diameter are 19 and 8 mm, respectively. They are widely used in cutting difficult-to-machine materials.
3. Force-measuring device. The force measuring system is composed by KISTLER Multi-component Force Plate Type 9253B23, Multichannel Charge Amplifier Type 5080 and DAQ for DynoWare Type 5697 that are made in Switzerland. The force measuring principle is shown in Fig. 2.
4. Test piece. A TC4-curved surface which is set as a test piece is a semicircular surface whose neutral surface radius is 20 mm, the designed thickness before finish machining is 800 μm, and the height is 20 mm. Flank milling method is adopted and the cutting thickness for both inner side and outer side of the curved surface is 300 μm, as shown in Fig. 3.

3.2 Establishment of cutting force model

The machining deformation of the thin-walled curved surface parts is mainly caused by cutting force [19], and the cutting force is related with the processing parameters, thus choosing proper processing parameters combination is of great importance. In order to predict the cutting force for simulation when the cutting parameters are determined, a cutting force model is required to be established.

In this study, response surface methodology (RSM), which is a kind of statistical method, is used to establish the cutting force model. The goal of RSM is to set up an approximate

Fig. 3 Test piece

function between input factors and output value by a series of experiments and statistic analysis. The related variables are put into action through a second-order polynomial expression with high efficient [20].

Box-Behnken design which is fit for three levels experimental design [21] is a commonly used one in RSM. It is a typical second-order model and can be carried out by the following steps. Firstly, a group of required data is gotten by designing certain experiments. Then, the multiple quadratic regression equation is adopted to satisfy the fitting function relation between factors and response value. Finally, the regression equation is established. Design-Expert Software (version 8.05b) is used in this study for the statistical design of experiments and data analysis.

As different parameters have different variation ranges and for the convenience of data processing, all the independent variables need a linear transformation, through which the problems caused by the difference of unit can be solved. The detailed step for encoding is as follows:

Set the actual data range of the ith variable X_i as $[X_{1i},X_{2i}]$, i= 1,2,…,m, at this time, the center point of this interval can be expressed as:

$$X_{0i} = \frac{(X_{1i} + X_{2i})}{2} \quad i = 1, 2, \ldots, m \tag{1}$$

The half length of the entire interval is:

$$\Delta i = \frac{X_{2i} - X_{1i}}{2} \quad i = 1, 2, \ldots, m \tag{2}$$

Repeat the linear transformation process for m times with the following equation:

$$x_i = \frac{X_i - X_{0i}}{\Delta i} \quad i = 1, 2, \ldots, m \tag{3}$$

In which, x_i is the encode value of each variable and is defined as factor level, X_i is the actual value of each variable, X_{0i} is the center point of the actual value for each variable, X_{1i} is the smallest actual value for each variable, X_{2i} is the largest actual value for each variable, and Δi is the difference value between two adjacent variables. After encoding, the actual variation range of X_i is changed into x_i, whose variation range is [−1, 1].

Considering that the allowance for finish machining is constant, three variables are taken into account. Based on the principle of RSM, three factors and three levels of response analysis method are adopted. The factors contain axial cutting depth, spindle speed, and feed speed which can be expressed as X_1, X_2, and X_3, respectively. The response value is the milling force that is perpendicular to the machining surface which can be expressed as Y. Synthesizing the cutting speed range of the milling tool and the high speed condition, the spindle speed is selected as 4000–6000 r min^{-1}. According to the recommended value studied before, the feed speed can be selected as 400–800 mm min^{-1}. In considering both efficiency and machining quality, the axial cutting depth can be selected as 0.5–1 mm. Calculated by Eqs. (1), (2), and (3), the corresponding relationship between actual factors value and the factor levels is shown in Table 1.

Table 1 Experimental factor coding level

Factor levels x	Factors		
	Axial cutting depth (a_p) X_1/mm	Spindle speed (n) X_2/ r min^{-1}	Feed speed (f) X_3/ mm min^{-1}
−1	0.5	4000	400
0	0.75	5000	600
1	1	6000	800

The experiment is organized by Box-Behnken design. After obtaining the response value (milling force) by force-measuring device as shown in Table 2, a multiple regression fitting can be gained.

The results satisfactorily fit a quadratic polynomial equation as described below in Eq. (4) by using coded factors:

$$Y = 41.60 + 4.77x_1 - 6.51x_2 + 5.57x_3 - 1.80x_1x_2 - 0.21x_1x_3 - 0.78x_2x_3 - 3.53x_1^2 - 5.34x_2^2 - 2.53x_3^2 \tag{4}$$

After replacing the coded factors by actual values, the predicted response value F can be expressed as:

$$F = -185.57 + 142.465 \times a_p + 0.054626 \times n + 0.12646 \times f - 0.0072 \times a_p \times n - 0.00425 \times a_p \times f - 3.8875 \times 10^{-6} \times n \times f - 56.56 \times a_p^2 - 5.34 \times 10^{-6} \times n^2 - 6.33125 \times 10^{-5} \times f^2 \tag{5}$$

Then, further optimization is carried out to determine the processing parameters combination. The results are as shown

Table 2 Box-Behnken design and corresponding responses

Series No.	x_1	x_2	x_3	Y
1	−1	−1	0	31.99
2	1	−1	0	47.55
3	−1	1	0	21.51
4	1	1	0	29.87
5	−1	0	−1	26.26
6	1	0	−1	33.80
7	−1	0	1	37.70
8	1	0	1	44.39
9	0	−1	−1	33.29
10	0	1	−1	22.90
11	0	−1	1	46.12
12	0	1	1	32.62
13	0	0	0	41.78
14	0	0	0	41.43

in Fig. 4. The contour line in the figure represents the variation tendency of the cutting force. What is more, the milling parameter will influence more about the milling force if the contour line is dense. Meanwhile, the closer to the red zone, the higher the milling force is. Thus, the milling force F increases with the increasing of axial cutting depth a_p and feed speed f and, to the contrary, decreases with the raising of spindle speed n. Furthermore, n has a bigger influence on cutting force because of the more intensive contour line which proves that the high speed milling is indeed suitable for thin-walled parts processing on account of its small milling force.

According to the date ranges of these three factors (spindle speed, feed per tooth, and cutting depth) and for the sake of reducing the milling force as well as improving the processing efficiency, choose a_p equals to 1 mm, n equals to 6000 r min^{-1}, and f equals to 400 mm min^{-1}. Plugging these parameters into Eq. (5) and the cutting force can be calculated as 21.91 N. The predicted milling force value can be used for machining deformation simulation.

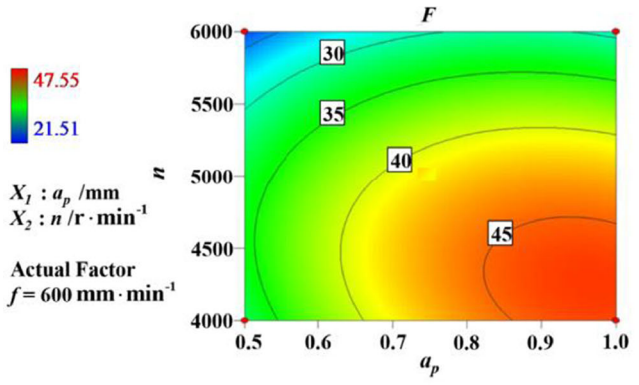

(a) n and a_p

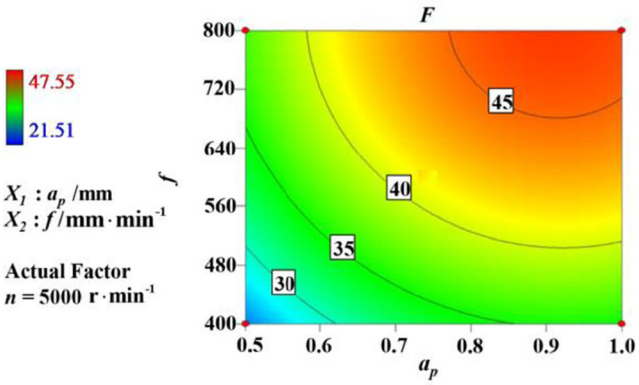

(b) f and a_p

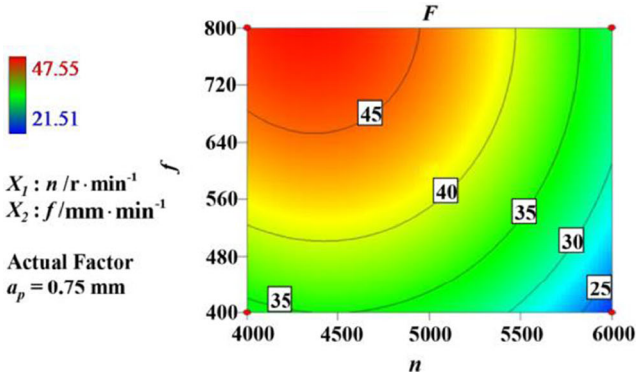

(c) f and n

Fig. 4 Relationship between variables and response values

3.3 Analysis for tool path planning

The rigidity of thin-walled parts is low. Meanwhile, for different positions of the part, the rigidity is changing a lot. Furthermore, as the rigidity is changing continuously along with the material removal process, different tool paths will lead to a different deformation degree. Hence, choosing an appropriate tool path is of vital importance.

Compared with the flat-shaped thin-walled structure, the arc-shaped one is more stable because of the structure that is similar to triangle, as shown in Fig. 5. When applying cutting force on point A, the material on AJ side and AC side will support force against the cutting force. When the material supply enough force to balance cutting force, the deformation will be small. However, when the cutting force is applied on the free end or near the free end such as point C and point J, in which condition the force supported by the material nearby cannot fight against the cutting force, the deformation emerges so as to reduce the material removal amount to reach a force balance. The same thing occurs in vertical direction of the arc-shaped thin-walled part. The total deformation value is the superposition of vertical direction deformation and the horizontal direction deformation. As seen in Fig. 6, the rigidity of position A is far larger than that of position C because position A is constraint by the material on both sides while position C is a free end. Based on the rigidity difference, two machining path strategies are proposed. Strategy I is to plan the machining tool path, as shown in Fig. 6a. Starting from position A, along with the path 1–2–3–4–5–6–7–8, a machining

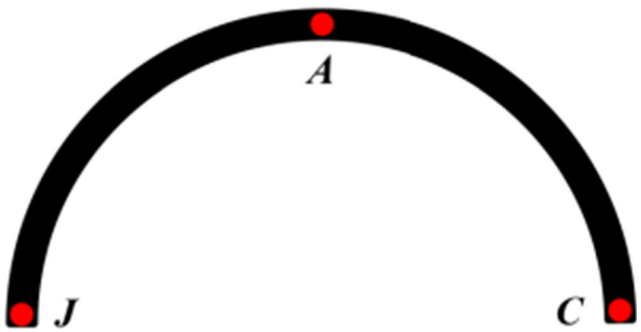

Fig. 5 Sketch map for deformation analysis in horizontal direction

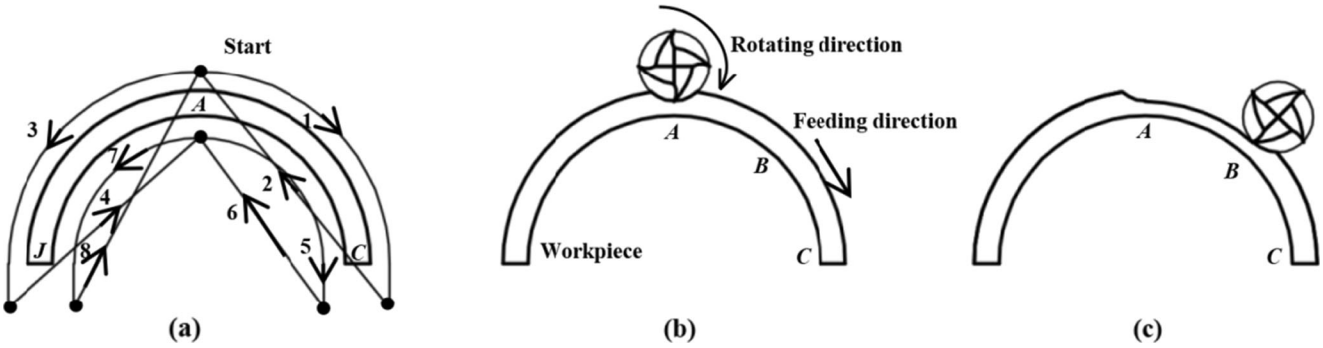

Fig. 6 Machining from high rigidity to low rigidity: **a** tool path, **b** start position, **c** machining direction

circulation is finished. Taking machining path I as an example, the machining starts from high rigidity position and ends at low rigid position; along with the cutting process, the thickness becomes smaller than before, which makes the rigidity reduce. As a result, the rigidity for position from point *A* to point *B* is close to that from point *B* to Point *C*, as shown in Fig. 6b, c. The rigidity balance guarantees a stable cutting process and reduces the fluctuation so as to decrease the machining deformation of the thin wall.

While strategy II is to plan the machining tool path, as shown in Fig. 7a, starting from position *C*, along with the path 1–2–3–4–5–6–7–8, a machining circulation is finished. Taking machining path II as an example, machining from point *C* to point *A*, in another word, moves from low rigidity position to high rigidity position; with the material removal as shown in Fig. 7b, c, the rigidity for the position from point *C* to point *B* becomes even smaller than that from point *B* to point *A*. The force fluctuation phenomenon becomes serious which leads to vibration and large deformation.

The above analysis for strategy II is under normal circumstance. However, on condition that the cutting tool is flaking because of the sudden collision against the part edge as shown in Fig. 8a, the material will be torn off instead of cutting off. Due to the small thickness of the part, edge failure phenomenon will occur because of the low strength, as shown in Fig. 8b. Therefore, this tool path is not available for high speed milling thin-walled parts. As a result, choosing strategy I for machining is reasonable.

3.4 Verification for tool path selection

The experiments show that when choosing strategy I for machining, the edge quality is good, as shown in Fig. 9a. However, it might be severely damaged when choosing strategy II, as shown in Fig. 9b. Thus, it is better to choose strategy I for machining. For the curved surface part machined with strategy I, the largest thickness difference is 104 μm by measuring.

3.5 Machining deformation estimation

Finite element simulation is an effective approach to predicted cutting deformation values without conducting experiments in advance. Thus, not only time but also materials and cutting tools can be saved so as to improve the efficiency a lot. In this study, ANSYS 14.0 is used to simulate the deformation of the TC4 arc-shaped thin-walled part. The necessary parameters are shown in Table 3.

The total thickness before cutting is 800 μm, and the cutting force perpendicular to the thin wall is 21.91 N when the cutting thickness is 300 μm according to the predicting result. The element type is selected as Solid185 which is a hexahedron element with eight nodes and 3DOF of displacement. The bottom of the curved surface part is fully constrained. The simulation result shown in Fig. 10 indicates that the biggest machining deformation is 36 μm under the condition of machining outer side of the thin wall. When machining the inner side, because of the material removal of the outer side, the deformation will be larger than that of the outer side

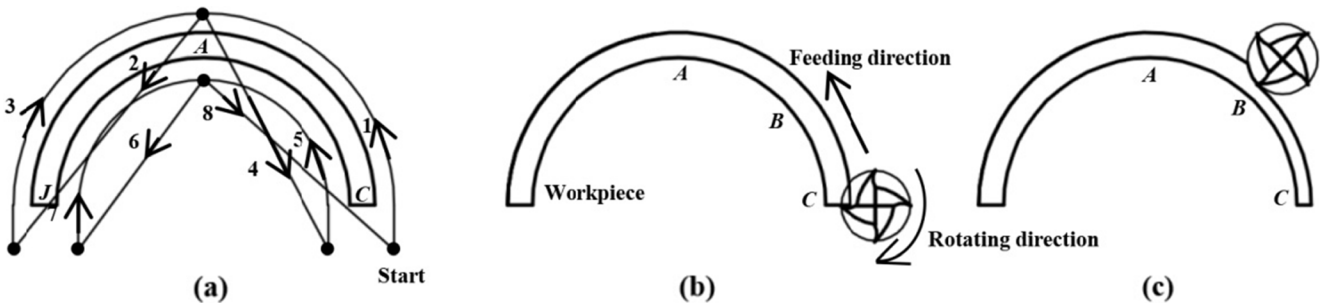

Fig. 7 Machining form low rigidity to high rigidity: **a** tool path, **b** start position, **c** machining direction

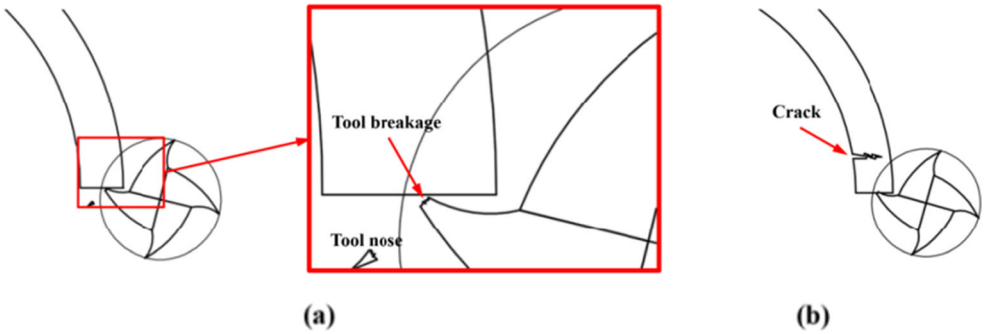

Fig. 8 Breakage formation sketch map: **a** partial enlarged view of the breakage, **b** crack

corresponding position. In this simulation, the influence caused by material removal is ignored and the deformation for inner side and outer side is regarded as symmetrical. Hence, the total deformation at the edge of the free end equals to a double of one side, namely equals to 72 μm.

Because of the material removal process, the rigidity is becoming smaller and smaller. Consequently, the actual machining deformation must be larger than the simulation one which ignores the rigidity variation related to material removal. What is more, by the effect of tool wear and some other factors which exist in actual machining, the deformation will also be larger than the simulated one. Hence, a coefficient must be multiplied to the simulated deformation value to make up for the impact of these factors. The results show that the largest actual machining deformation is 104 μm, and the simulated deformation is 72 μm. As a result, the coefficient λ can be calculated as 1.4, according to the actual machining deformation and the simulated deformation.

After obtaining this coefficient, the actual machining deformation can be predicted by the simulated value; thus, it is no need to do a try-cut in advance which makes the working efficiency improve significantly.

4 Machining deformation compensation

In this section, a compensation approach is proposed to guarantee the shape precision of the difficult-to-machine material thin-walled parts with curved surface.

4.1 Principle of compensation method

Aiming at the cutting deformation of the difficult-to-machine material thin-walled parts with curved surface, a mirror compensation method is proposed to reduce the degree of deformation. The meaning of mirror compensation is that the compensation value equals to the deformation value, as shown in Fig. 11. With the following schematic diagram, the principle of mirror compensation method can be explained as follows. The continuous thin lines represent the designed profile which is willing to be obtained. The dotted lines represent the actual machined profile with the deformation error. The continuous thick lines represent the desired machining profile with compensation. At corresponding position, the distance between the continuous thick line and the continuous thin line, namely the compensation value, equals to the distance between the continuous thin line and the dotted line, namely the deformation error value. The compensation procedure is carried out based on this mirror compensation principle.

4.2 Compensation algorithm of machining deformation

The total deformation is overlaid by the vertical deformation and the horizontal deformation. Hence, calculate the vertical free end deformation first and then use it to calculate the horizontal deformation. According to the measurement data of the uncompensated part, the vertical direction thickness difference is expressed as t_θ. As the vertical direction is a straight wall and the horizontal direction is a semicircle which is a quadratic curve, hence, the thickness variation for the vertical direction and horizontal direction can be regarded as the linear and the quadratic relation, respectively. Thus, the unit compensation value on vertical edge Δt_θ can be expressed as:

$$\Delta t_\theta = \frac{t_\theta}{2 \times n} \tag{6}$$

where n represents the milling cycles.

Thereby, the compensation value for different positions can be calculated as follows:

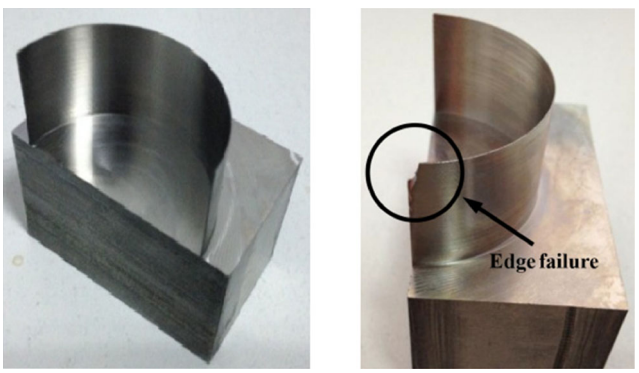

Fig. 9 Comparation between two tool paths: **a** from high rigidity to low rigidity, **b** from low rigidity to high rigidity

Table 3 Composition and mechanical properties of TC4

Content of TC4	Al	V	Fe	O	C	N	H	Ti
Composition (wt%)	6.2	3.9	0.16	0.14	0.023	0.018	–	Balance
Workpiece material	Yield strength (MPa)	Tensile strength (MPa)	Hardness (HRC)	Elongation (%)	Young's modulus(GPa)			
TC4	925	970	38	11	110			

$$\begin{cases} \Delta_1 = \Delta t_{\theta_1} h = a_1(\theta_3 - \theta_1)^2 + a_2(\theta_3 - \theta_1) \\ \Delta_2 = \Delta t_{\theta_2} h = a_1(\theta_3 - \theta_2)^2 + a_2(\theta_3 - \theta_2) \end{cases} \tag{7}$$

where Δ_1 represents the compensation value for each cutter location points at position K, Δ_2 represents the compensation value for each cutter location points at position P in Z-axis direction in the space coordinate system, h represents the distance between cutting position and the bottom of the thin wall, a_1 and a_2 are the coefficients of the quadratic equation, θ_1 represents the angle between X-axis and line OK in horizontal coordinate system, θ_2 represents the angle between X-axis and line OP in horizontal coordinate system, and θ_3 represents the angle between the thickness changing position OQ and X-axis as shown in Fig. 12.

Through replacing the coefficient by the measurement data, the equation set can be worked out. Thus, the compensation value Δ can be calculated. Then, the compensated cutter location point (x, y) in X-O-Y coordinate system can be obtained as follows:

$$\begin{cases} x = L \times \cos\theta \\ y = L \times \sin\theta \end{cases} \quad \theta \in [0, \theta_3] \tag{8}$$

where θ represents the angle between MO and X-axis as shown in Fig. 13, L is the actual distance from cutting point (x, y) to original point O, which can be expressed as:

$$L = R \mp \frac{d}{2} \pm \Delta \tag{9}$$

where R represents the neutral plane radius of the part, d represents the designed thickness of the thin wall; select '–' when machining the outer contour and '+' when machining the inner contour.

Set the cutter location point before compensation as (x_1, y_1) and it can be obtained by

$$\begin{cases} x_1 = R \times \cos\theta \\ y_1 = R \times \sin\theta \end{cases} \quad \theta \in [0, 90] \tag{10}$$

By substituting Eqs. (8) and (9) into (10), it can be obtained that:

$$\begin{cases} \dfrac{x_1}{R} = \dfrac{x}{R \mp \dfrac{d}{2} \pm \Delta} \\ \dfrac{y_1}{R} = \dfrac{y}{R \mp \dfrac{d}{2} \pm \Delta} \end{cases} \tag{11}$$

Thus:

$$\begin{cases} x = \dfrac{x_1 \times \left(R \mp \dfrac{d}{2} \pm \Delta\right)}{R} \\ y = \dfrac{y_1 \times \left(R \mp \dfrac{d}{2} \pm \Delta\right)}{R} \end{cases} \tag{12}$$

Consequently, the compensated cutter location point (x, y) can be obtained by substituting the original one (x_1, y_1) into Eq. (12).

5 Verification experiment

Replacing all the coefficients by measurement data of the uncompensated part which are shown in Fig. 14, the thickness

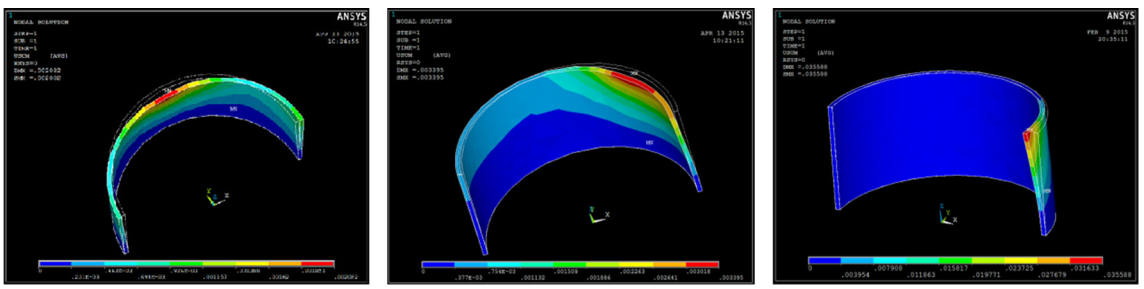

(a) (b) (c)

Fig. 10 ANSYS simulation result. **a** Loading at symmetrical position. **b** Loading at 45° direction. **c** Loading at the free end

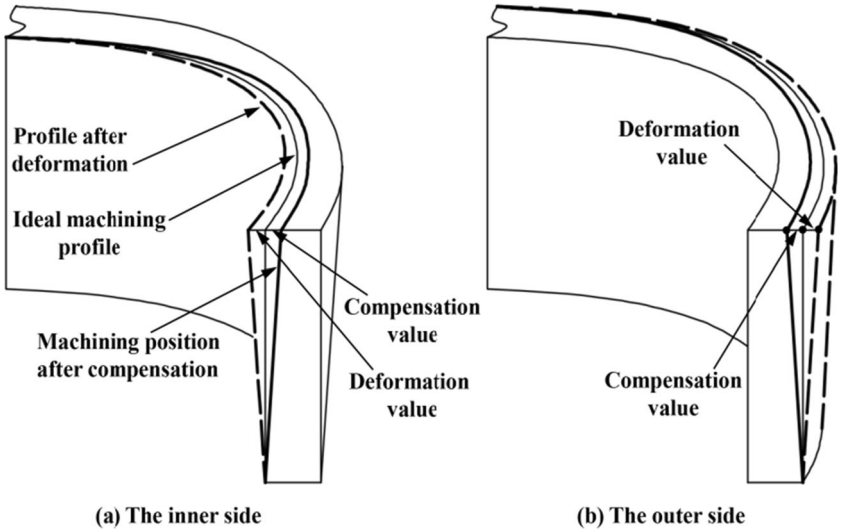

Fig. 11 Mirror compensation principle

difference is 104 μm. The axial cutting depth is 1 mm, and the height of the arc-shaped thin-walled part is 20 mm; therefore, 20 times cutting circulation will be carried out to finish the whole process. After calculating, the unit compensation value on vertical edge is 2.6 μm and that for section cutting plane at position P is 0.66 μm for one milling cycle. The thickness becomes unchangeable when θ is larger than 45°. Hence, θ_3 equals to 45°.

Thereby, the equation can be calculated as:

$$\begin{cases} \Delta_1 = 2h = a_1(45-\theta_1)^2 + a_2(45-\theta_1) \\ \Delta_2 = 0.66h = a_1(45-\theta_2)^2 + a_2(45-\theta_2) \end{cases} \quad (13)$$

According to the measurement result shown in Fig. 14, it can be seen that θ_1 equals to 0° and θ_2 equals to 15°. Thus Eq. (13) can be expressed as:

$$\begin{bmatrix} 900 & 30 \\ 2025 & 45 \end{bmatrix} \begin{bmatrix} a_1 \\ a_2 \end{bmatrix} = \begin{bmatrix} 0.66h \\ 2.6h \end{bmatrix} \quad (14)$$

The solution is:

$$\begin{bmatrix} a_1 \\ a_2 \end{bmatrix} = \begin{bmatrix} 2.4 \times 10^{-3}h \\ -0.05h \end{bmatrix} \quad (15)$$

As a result, the equation for calculating the compensation value in X-O-Y coordinate system is shown as:

$$\Delta = 2.4 \times 10^{-3}h(45-\theta)^2 - 0.05h(45-\theta) \quad h = 0, 1, 2, \ldots, 19 \quad (16)$$

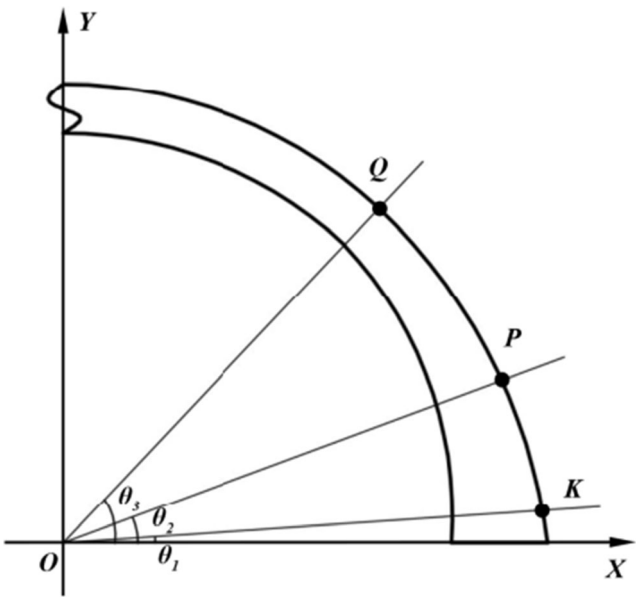

Fig. 12 Cutter location calculating mechanism

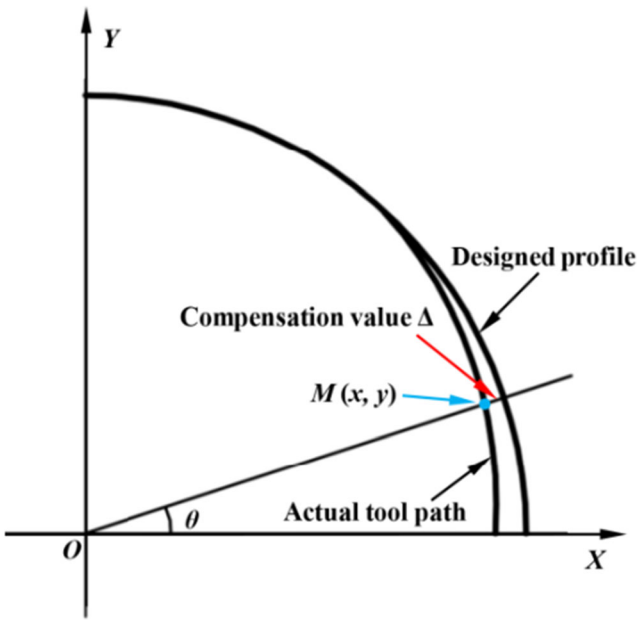

Fig. 13 Principle of cutter location point compensation

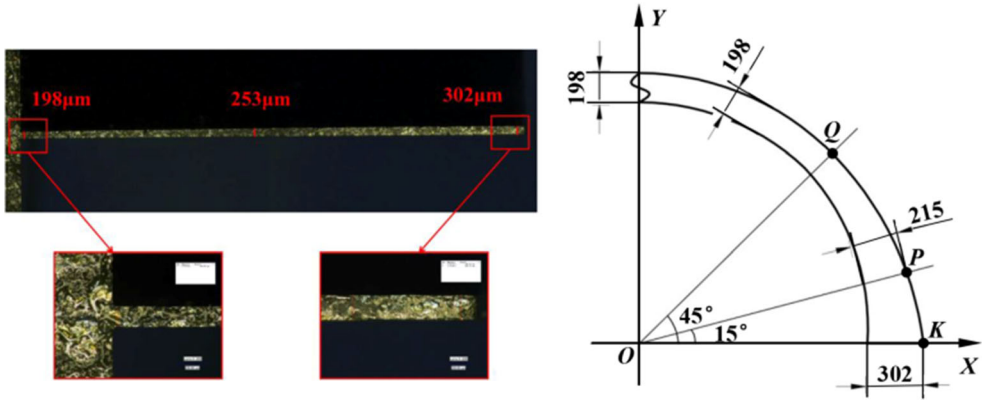

Fig. 14 Thin wall thickness without compensation

For the experimental part, R equals to 20 mm and d equals to 200 μm. Taking Δ into Eq. (12), it can be obtained that:

$$\begin{cases} x = \dfrac{x_1 \times \left(20 \mp 0.1 \pm 2.4 \times 10^{-3} h(45-\theta)^2 - 0.05h(45-\theta)\right)}{20} \\ y = \dfrac{y_1 \times \left(20 \mp 0.1 \pm 2.4 \times 10^{-3} h(45-\theta)^2 - 0.05h(45-\theta)\right)}{20} \end{cases} \tag{17}$$

Once the original cutter location point (x_1, y_1) is obtained, the compensated cutter location point (x, y) can be worked out. MATLAB is used to complete the calculation process.

The verification experiment is conducted with the compensated cutter location points. The results shown in Fig. 15 indicate that the largest thickness difference after compensation is 49 μm, which is reduced by 52.88 % compared with the former 104 μm. Meanwhile, the percentage has a decreasing tendency with the increasing of the wall thickness.

6 Conclusions

This paper presents an effective approach for reducing machining deformation based on the rigidity change in the process of machining difficult-to-machine material thin-walled parts with curved surface. According to the findings of this study, some conclusions are as follows:

1. With the increasing of the spindle speed, the cutting force has a decreasing tendency, while with the growth of feed speed and axial cutting depth, the cutting force displays an increasing tendency. Otherwise, the spindle speed has a more obvious influence on cutting force. Therefore, a group of parameters which contains a lower feed speed but a higher spindle speed is selected for thin-walled curved surface parts milling.
2. The tool path that starts processing from high rigidity position and ends at low rigidity position can effectively

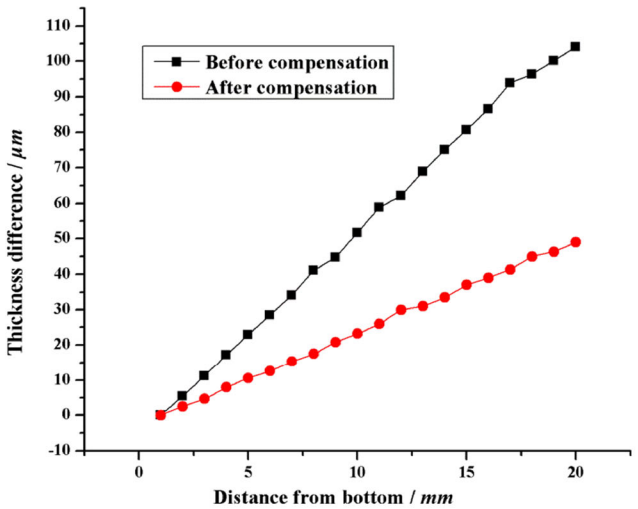

(a)

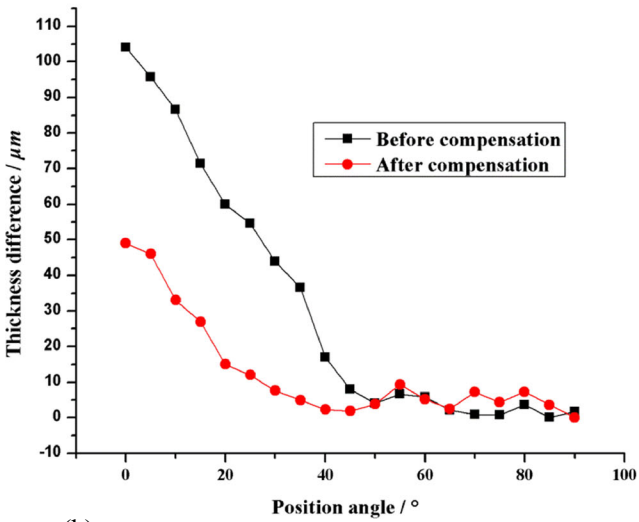

(b)

Fig. 15 Comparation for the compensated value and the uncompensated value. **a** Thickness difference in vertical direction. **b** Thickness difference in horizontal direction

reduce the cutting deformation. Meanwhile, it makes the cutting process more stable and avoids the tools from being damaged.

3. The coefficient is obtained as λ equals to 1.4 according to the simulation deformation result 72 μm and the actual compensation deformation result 104 μm. With this coefficient, the compensation value can be predicted without conducting an experiment in advance. Therefore, large amount of time and material can be saved, which improves the processing efficiency significantly.
4. The machining deformation compensation is based on cutter location point modification method. Once the original cutter location point is obtained, the compensated one can be worked out easily.
5. Mirror compensation method is adopted. By conducting validation experiment, it can be seen that the largest thickness difference is 104 μm before compensation, while it reduces to 49 μm after compensation, which indicates that the deformation degree decreases by 52.88 % after adopting the proposed compensation method when the thin wall thickness is 200 μm.

The achievements of this research are of vital importance for improving the machining quality of difficult-to-machine material thin-walled parts with curved surface and the solving method can be generalized to the machining of ordinary thin-walled curved surface parts used in aerospace industry.

Acknowledgments The project is supported by the National Natural Science Foundation of China (no. 51575087, 51205041), Science Fund for Creative Research Groups (no. 51321004), Basic Research Foundation of Key Laboratory of Liaoning Educational Committee (no. LZ2014003), Open Research Fund of Key Laboratory of High Performance Complex Manufacturing (no. Kfkt2013-06), and the Fundamental Research Funds for the Central Universities (no. DUT14QY25, DUT14RC(4)16). The authors wish to thank the anonymous reviewers for their comments which led to improvements of this paper.

References

1. Jin Q, Liu SG (2007) Optimization of fixture scheme for milling thin-walled arc workpiece. Tool Eng 41(12):54–57
2. Abdolvand H, Sohrabi H, Faraji G, Yusof F (2015) A novel combined severe plastic deformation method for producing thin-walled ultrafine grained cylindrical tubes. Mater Lett 143:167–171
3. Wang ZG, Rahman M, Wong YS (2005) Tool wear characteristics of binderless CBN tools used in high-speed milling of titanium alloys. Wear 258(5–6):752–758
4. Liu WW, Zhang DH, Shi YY, Ren JX, Wang WH (2004) Study on net-shape NC machining technology of thin-blade of aero-engine. J Mech Sci Technol 23(3):329–331
5. Wang YQ, Mei ZY, Fan YQ (2004) Nonlinear finite element analysis of deformation in machining of thin-wall arc shaped workpiece. Aeronaut Manuf Technol 6:84–86
6. Alinia MM, Dastfan M (2006) Behaviour of thin steel plate shear walls regarding frame members. J Constr Steel Res 62(7):730–738
7. Andris L, Toms T (2015) The influence of high-speed milling strategies on 3D surface roughness parameters. Procedia Eng 100: 1253–1261
8. Smith S, Dvorak D (1998) Tool path strategies for high speed milling aluminum workpiece with thin webs. Mechatronics 8(4):291–300
9. Iwabe H, Mizuochi M, Yokoyama K (1999) High accurate machining of thin wall shape workpiece by end mill. Proposal of twin spindle type machining and some experiments. Trans JSME A 65(632):1719–1724
10. Ratchev S, Liu S, Becker AA (2004) Milling error prediction and compensation in machining of low-rigidity parts. Int J Mach Tool Manuf 44(15):1629–1641
11. Chen WF, Xue JB, Tang DB, Chen H, Qu SP (2009) Deformation prediction and error compensation in multilayer milling processes for thin-walled parts. Int J Mach Tool Manuf 49(11):859–864
12. Nedelcu M, Cucu HL (2014) Buckling modes identification from FEA of thin-walled members using only GBT cross-sectional deformation modes. Thin Wall Struct 81(SI):150–158
13. Vetyukov YM (2010) Theory of thin-walled rods of open profile as a result of asymptotic splitting in the problem of deformation of a noncircular cylindrical shell. J Elast 98(2):141–158
14. Izamshah R, Mo JPT, Ding S (2012) Hybrid deflection prediction on machining thin-wall monolithic aerospace components. Proc Inst Mech Eng B J Eng 226(B4):592–605
15. Papastathis TN, Ratchev SM, Popov AA (2012) Dynamics model of active fixturing systems for thin-walled parts under moving loads. Int J Adv Manuf Technol 62(9–12):1233–1247
16. Liu G (2009) Study on deformation of titanium thin-walled part in milling process. J Mater Process Technol 209(6):2788–2793
17. Arnaud L, Gonzalo O, Seguy S, Jauregi H, Peigné G (2011) Simulation of low rigidity part machining applied to thin-walled structures. Int J Adv Manuf Technol 54(5–8):479–488
18. Tang ZT, Yu T, Xu LQ, Liu ZQ (2013) Machining deformation prediction for frame components considering multifactor coupling effects. Int J Adv Manuf Technol 68(1–4):187–196
19. Wojciechowski S (2015) The estimation of cutting forces and specific force coefficients during finishing ball end milling of inclined surfaces. Int J Mach Tool Manuf 89:110–123
20. Han HZ, Li BX, Wu H, Shao W (2015) Multi-objective shape optimization of double pipe heat exchanger with inner corrugated tube using RSM method. Int J Therm Sci 90:173–186
21. He W, Xue WD, Tang B (2012) Optimization design of experiment method and data analysis. China Chemical Industry Press, Beijing